OPTICAL FIBER TECHNOLOGY **1,** 283–288 (1995)

Evaluation of New UV-Curable Adhesive Material for Stable Bonding between Optical Fibers and Waveguide Devices: Problems in Device Packaging

HIROTOSHI NAGATA, MASARU SHIROISHI, YASUYUKI MIYAMA, NAOKI MITSUGI, AND NOBUHIDE MIYAMOTO

Optoelectronics Division of the Central Research Laboratories, Sumitomo Osaka Cement Co., Ltd., 585 Toyotomi-cho, Funabashi-shi, Chiba 274, Japan

Received February 3, 1995

In a hermetically sealed package ef waveguide devices, optical fibers are bonded to the waveguide terminal with resin adhesive materials. Here, a recently deveioped commercial epoxybased, ultraviolet-radiation-curable adhesive material with a low refractive index of 1.46 is evaluated for such a purpose where chemical and mechanical stability and reliability are greatly demanded. The results show this adhesive material exhibits reliable bonding characteristics for the fiber and Ti:$LiNbO_3$ waveguide with high chemical stability, indicating its possibile application in packaged components for optical communication systems.

1. INTRODUCTION

Waveguide devices such as high speed Ti:$LiNbO_3$ optical modulators need to be connected with the optical fibers in hermetically sealed packages to achieve stable and reliable operation in optical communication systems. A mechanically rigid bonding with adhesive materials is one way to make such a connection. The adhesive materials for such optical uses need to have a low refractive index, close to that of the optical fiber, to reduce return losses of the propagating lightwave at the bonded interface. Furthermore, ultraviolet-radiation- (UV) curable materials which need only a few minutes to solidify are suitable to eliminate optical insertion losses due to unexpected disalignment between the fiber and waveguide during the long-time curing process. In this regard, some UV-curable adhesive materials with a refractive index of ~ 1.56 are commercially supplied and have been conventionally used exhibiting high reliability. One such typical material, "*N*," was analyzed to be composed of triallyl isocyanurate as a polyene, pentaerythritol tetramercaptopropinate as a thiol, and benzophenone as a photoinitiator. However, UV-curable materials with further low refractive indices are preferable to greatly decrease optical losses of the assembled devices. A group at NTT Co. reported originally on fluoridated epoxybased UV-curable materials whose refractive indices changed from 1.59 to 1.45 in proportion to the increase of the fluorine contents (in wt%) in them [1]. Recently, Daikin Industries, Ltd. has supplied commercially such adhesive materials with refractive indices of less than 1.5 [2]. Here, among Daikin's commercial materials, the one labeled as UV-1100 is evaluated by us and reported on from the viewpoints of its chemical and mechanical stabilities for usage in hermetically sealed waveguide devices. The results suggest that this UV-1100 adhesive can bond the fiber and waveguide terminals, which are to be exposed under ordinary device operating temperatures between 0 and 70℃.

2. GENERAL CHARACTERISTICS OF THE UV-1100 ADHESIVE

The technical catalog of the UV-1100 adhesive denotes its characteristics as follows: the main content is an epoxy with viscosity, specific gravity, and refractive index of 250 cps, 1.36, and 1.435 at 25℃, respectively, before solidification. After solidification by 10 J/cm^2 radiation with a high-pressure Hg lamp, the specific gravity and refractive index change to 1.42 and 1.458 (1.453 at 70℃), respectively. The mass contraction due to solidification is 4–5%. The glass transition temperature T_g is 145℃, judging from tan δ in kinetic viscoelasticity measurement. The moisture absorbency at 85℃ and 85% RH is saturated at 2.4 wt%.

The characteristics of the solidified UV-1100 material did not deteriorate as a result of high temperature storage at 120℃ for 100 h and 100 heat cycles between –40 and 85℃ (90% RH). The refractive index and optical transparency (sample thickness = 0.1 mm and lightwave length = 1.3 μm) were 1.455 and 94.2% after the 120℃ storage, and 1.456 and 94.2% after the heat cycles, respectively. The bonding strengths were confirmed to be greater than ~ 70 Kg/cm^2 of bonded glass samples (1 × 2 cm^2), even after the above environmental tests.

3. CURING CONDITIONS

The curing process for the UV-curable materials consists

1068-5200/95 $6.00

of a rapid polymerization induced by UV-reactive photoinitiators and a succeeding slow thermal polymerization. For the UV-1100 adhesive material, a postcuring treatment at 60℃ is recommended after the UV-curing treatment. Here, a temperature dependency of the polymerization was investigated to determine the proper curing temperature experimentally. The UV-1100 liquid was spread ~ 20 mm in diameter and ~ 1 mm thick on a Teflon board. This was cured for 4 min with 50 mW/cm^2 of UV-light radiated from a Hg-lamp. The solidified UV-1100 disks were postcured immediately for 60 min at 60, 80, or 90℃ using an oven. These treatments were carried out in a room where the humidity was controlled at less than 40%. If the UV-curing was conducted under higher humidity conditions, the color of the solid tended to become turbid. These samples are denoted here as "A" for the one without any postthermal curing, "B" for the one postcured at 60℃, "C" for the one cured at 80℃, and "D" for the one cured at 90℃. All samples were stored with silica gel to decrease their possible moisture absorption.

Differential scanning calorimetry (DSC) measurement was carried out on all samples from 30 to 250℃ with a heating rate of 10℃/min under N_2 environment. Figures 1a, 1b, 1c, and 1d show the DSC results of samples A, B, C, and D, respectively. The non-postcured sample A exhibited a larger calorific value of 64 J/g than the others (B, 40 J/g; C, 39 J/g; D, 34 J/g). The starting and peak temperatures of these exothermic reactions, which possibly came from thermal polymerization, were measured as 60℃ (start) and 94℃ (peak) for A, 70 and 110℃ for B, 70 and 108℃ for C, and 70 and 112℃ for D. The end temperature of the reactions was 205–220℃. These results indicate that the remaining polymerization (solidification) of the UV-cured sample included at least two processes, and one of them was possibly accomplished via the postcuring treatment at 60℃. In order to further enhance the reactions, the heat treatment over 100℃ was necessary. However, since the high-temperature process was disadvantageous for other device materials such as optical fiber jackets, the postthermal curing temperature of 60℃ was acceptable. It was noted that the UV-1100 liquid without any UV-curing treatment was not solidified by the heating only and exhibited no DSC peak because of a possible lack of reactive cation species.

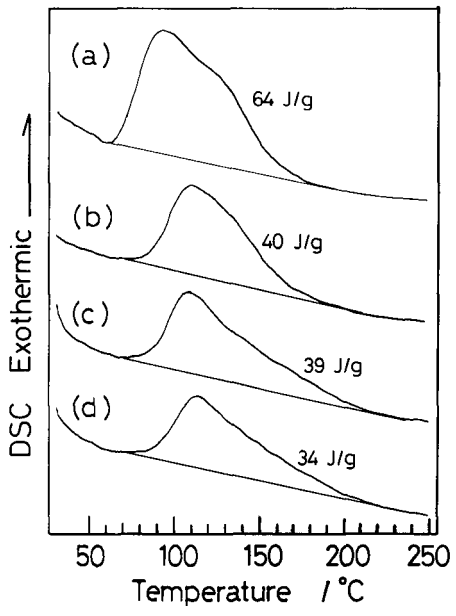

FIG. 1. Results of DSC measurements of UV-cured UV-1100 adhesive materials without postthermal curing (Sample A) (a) and with postthermal curing for 1 h at 60℃ (Sample B) (b), 80℃ (Sample C) (c), and 90℃ (Sample D) (d). The exothermic peaks were attributed to thermal polymerization.

Figure 2 shows the typical DSC result of the completely polymerized material A which was previously heated to 250℃. The observed step-like endothermic peak denotes the T_g of the material. The result similarly measured for the sample C was almost the same, and starting and ending temperatures of the glass transition were measured at 109–111℃ and 142–145℃, respectively, which agreed well with the 145℃ derived from a viscoelasticity measurement.

To compare degrees of the polymerization depending on the curing temperatures, Fourier transform infrared spectroscopy (FTIR) measurement was made for samples A–D and the sample C which had been previously heated to 250℃ and completely polymerized. Figure 3 exhibits these results and the peak at 860 cm^{-1} specifically depending on the sample treatment procedure. This peak, ascribed possibly to an epoxy ring, indicates the degree of the polymerization, judging from its extinction in the completely polymerized sample (Fig. 3e). The peak intensities observed in Figs. 3a–3d, corresponding to samples A–D, suggested the degrees of polymerization (solidification) of the materials as A < B ≤ C ≤ D. This result was similar to the above-mentioned DSC data and supported again setting the postcuring temperature at 60℃.

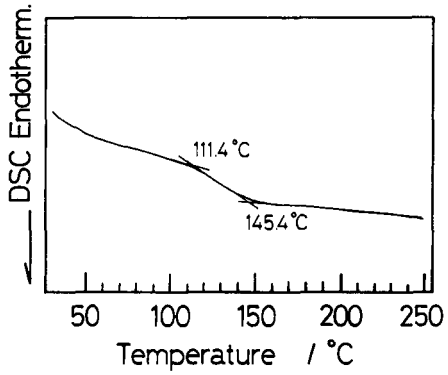

FIG. 2. DSC result of sample A measured after the UV-curing and postheating to 250℃. The endothermic peak corresponds to the glass transition temperature of the solidified UV-1100 material.

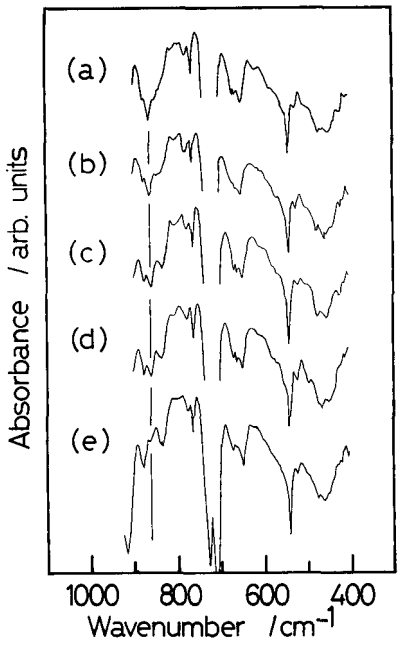

FIG. 3. FTIR spectra of UV-1100 sample A (a), B (b), C (c), and D (d). The spectrum (e) is for the sample C which was heated to 250℃ in addition to being postthermal cured at 80℃.

4. CHEMICAL STABILITY

Prior to evaluation of the chemical stability of the solidified UV-1100 material, its chemical composition was analyzed before solidification by gas chromatography (GC), GC accompanied with mass spectroscopy (GCMS), FTIR, ^{1}H-nuclear magnetic resonance (NMR), and ^{13}C-NMR methods. There remained a few unknown fragments, possibly polyvinylidene fluoride, and other fragments could be identified as aliphatic or alicyclic compounds containing only epoxy radicals, vinylcyclohexanedioxide and bisphenol A type epoxy.

Figures 4a–4d are the results of thermogravimetry (TG) for samples A–D measured from 30 to 200℃ with a heating rate of 10℃/min under flowing He. Their weight losses were similar and measured at 200℃ to be 0.20% for A, 0.31% for B, 0.21% for C, and 0.22% for D. The water amounts evaporated from the sample B were measured at 80℃ to be 0.12 wt% and at 200℃ to be 0.24 wt% by a Karl Fischer technique, indicating that the observed thermal weight losses of the solidified UV-1100 material were due to evaporation of the included water. The volume of the adhesive material used in the device package for bonding fibers is significantly small. If several UV-1100 drops with ~ 0.5 mm diameter were used for the bonding, the weight of the solidified material was estimated at less than l mg. Therefore, the increase of water content in the package due to the UV-1100 material at 80℃ of ordinary device storage temperature was less than 1 ppm.

The decomposition of the solidified UV-1100 material was measured by a TG-GCMS technique up to 200℃ under a He

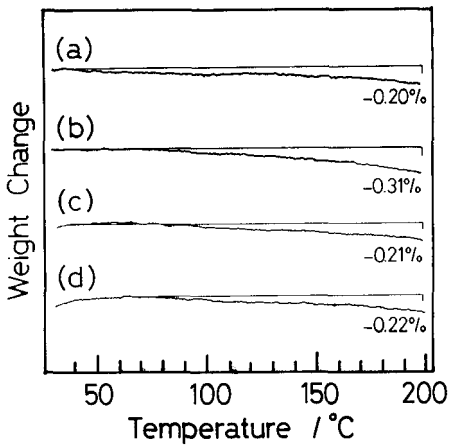

FIG. 4. TG profiles of UV-1100 samples A (a), B (b), C (c), and D (d). The observed weight losses are almost the same as those due to evaporation of included water.

atmosphere. From sample A with only UV-curing, there appeared evaporated fragments such as formaldehyde, methanol, acetoaldehyde (or oxirane), propanal (and/or propenal), carbon disulfide + propanal and/or propenal, benzene, toluene, xylene, and styrene. The fragments from "formaldehyde" to "propanal" could have onginated from the epoxy compound. The other fragments could have come from a UV-decomposed photoinitiator which was identified as an aromatic sulfonium compound. In the measurements for the postthermal cured samples B, C, and D, a broad unknown peak and a peak for diphenyl sulfide were additionally detected. Figure 5 shows the TG-MS results for sample B as a relationship between the peak intensities of the above-men-

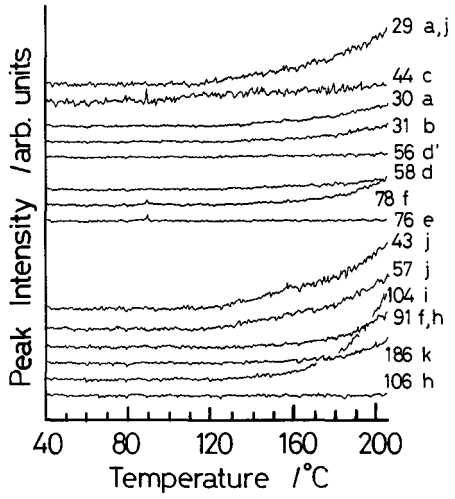

FIG. 5. TG-MS profiles of the UV- 1100 sample B which was conveniently postthermal cured at 60℃ for 1 h. Numerical values denote the mass numbers of detected fragments. These fragments were attributed to (a) formaldehyde, (b) methanol, (c) acetoaldehyde or oxirane, (d) propanal and/or propenal, (d') 2-propenal, (e) carbon disulfide, (f) benzene, (h) xylene, (i) styrene, (j) unknown compounds, and (k) diphenyl sulfide.

tioned fragments and temperature. At ~ 90℃, the evaporation of acetoaldehyde (or oxirane) started (see the curve "44 c" of Fig. 5) while others evaporated over 100℃, indicating the high chemical stability of the UV-1100 material within the ordinary device operating temperature range.

5. MECHANICAL STABILITY

The temperature dependency of the bonding strength of the UV-1100 adhesive was investigated. On a polished $LiNbO_3$ surface, a SiO_2 glass bead with ~ 1 mm outer and ~ 0.15 mm inner diameters was bonded using the UV-1100 (postthermal curing temperature was 60℃). Similar specimens were prepared using a conventional UV-curable adhesive material *N* (mentioned in Section 1). All 20 sets of specimens were placed in an oven while a force of 37 g was applied to each specimen along the bonding face (i.e., a direction of the shearing force). Figure 6 shows the numbers of the unfailed specimens at various temperatures for 30 min. Open and closed circles denote the results for the UV-1100 and the conventional *N* adhesives, respectively. Although the UV-1100 exhibited lower temperature endurance than the *N*, it was found to be applicable for the uses below 80℃. In practical device packages, such a large force should not be applied continuously to the bonded fibers. The shearing strengths measured for specimens similar to the UV-1100 were 850 g on average (standard deviation = 150 g) as-prepared, 1700 g (480 g) after a 130℃/30 min storage, and 1100 g (330 g) after a 150℃/5 min storage. Such deterioration and broad distribution of the bonding strengths at higher temperatures were possibly due to the, competition of thermal polymerization and decomposition observed beyond 90℃ (mentioned in Section 4).

6. APPLICATION OF UV-1100 TO DEVICE ASSEMBLY

The UV-1100 adhesive was used here to bond the optical fiber to the waveguide terminal of a Ti:$LiNbO_3$ Mach–Zehnder optical intensity modulator. The structure of this bonding is schematically shown in Figs. 7a and 7b, where a $LiNbO_3$ block and a 1- to 1.5-mm-long SiO_2 glass bead were also bonded for reinforcement. The size of the modulator chip terminal, including the block, was 0.8×1 mm^2 while the outer diameter of the bead was 1 mm. The fiber terminal was cleaved normal to the axis. The $LiNbO_3$ chip and the bead were cut having specific small slant angles against their axes to keep the fiber leaning 2° from the Ti:$LiNbO_3$ waveguide axis, reducing the possible back-reflection of the propagating light (wavelength = 1.5 μm). The postthermal curing temperature was 60℃. When the postcuring was done at 90℃, two of four such treated devices failed due to their optical loss increases during the curing process. This $LiNbO_3$/fiber component was hermetically packed with dry N_2/He (a dew point < –35℃) in a stainless steel package, where a He leak rate less than 5×10^{-8} atm cm^3/s was maintained.

To know the mechanical stability of the bonding, the changes of optical insertion losses of 118 modulator devices were investigated after sequential environmental tests of 100-h storages at 80℃ and 20 heat cycles between –20 and 70℃ (rate ≃ ± 2℃/min and soaking ≃ 30 min). Measurements of the optical insertion losses were made at room temperature. Some modulator samples consisted of an Al/SiO_2 laminated polarizor which was inserted between the waveguide terminal and fiber and also bonded with the UV-1100. The results are plotted by open circles in Figs. 8a and 8b, as the distribution *f* (%) versus loss change values in Fig. 8a and as its cumulative distribution *F*(%) in Fig. 8b. The reasons for

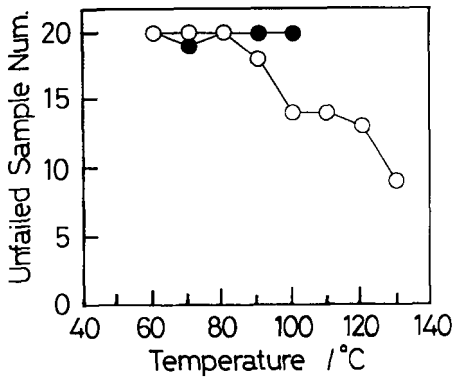

FIG. 6. Numbers of the unfailed specimens after 30 min storage at various temperatures, prepared by bonding the 1-mm-diameter glass bead to the $LiNbO_3$ substrate with the UV-1100 (open circles) and the conventional adhesive material *N* (closed circles). During storage, a load of 37 g was applied to the shearing direction for the bonded interface. The sample number for each of the tests was 20.

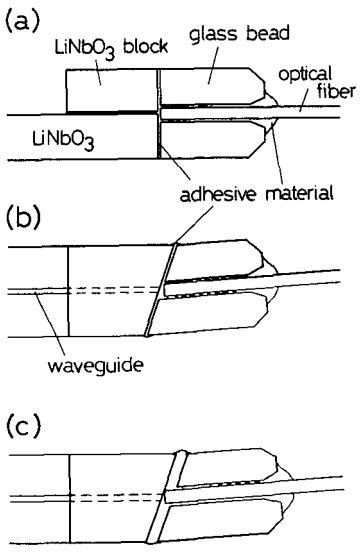

FIG. 7. Schematic illustrations of bonding structure of the optical fiber to the Ti:$LiNbO_3$ waveguide using the $LiNbO_3$ block and the glass bead for the bonding strength reinforcement. The structure, presented as cross section (a) and as top view (b), is considered to be highly reliable and is used here for the modulator sample preparation. The structure shown in (c) is the alternative one. The glass beads in the illustrations are shown as the cross section.

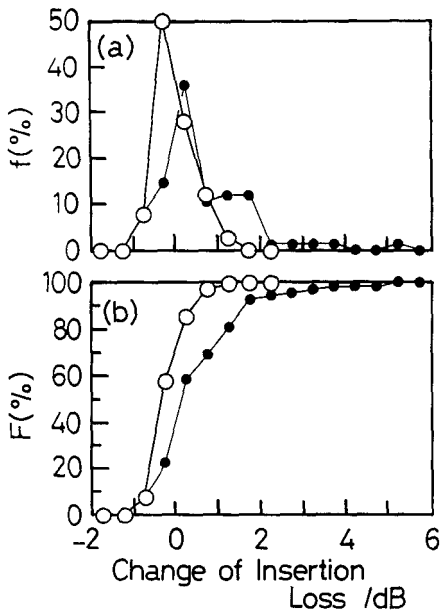

FIG. 8. (a) The distribution f (%) of the optical insertion loss changes in the fabricated devices due to sequential environmental tests of the 80℃ storage for 100 h and the 20 heat cycles between –20 and 70℃. The detected loss changes seemed to originate from the points where the optical fibers were bonded to the Ti:$LiNbO_3$ waveguides with the UV- 1100 adhesive material (postcuring at 60℃). (b) The cumulative distribution F (%) of the same results. Open circlcs denote results for 118 modulator samples consisting of the bonding structure shown in Figs. 7a and 7b. Closed circles denote results for 78 samples fabricated as in Fig. 7c.

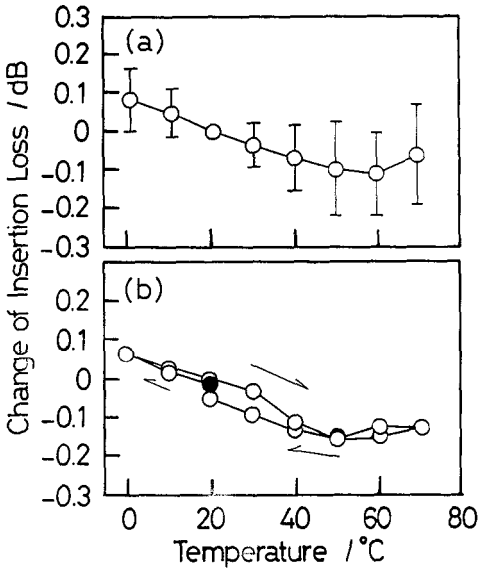

FIG. 9. Temperature dependence of the optical insertion loss changes for the modulator samples fabricated as in Figs. 7a and 7b. The error bars of (a) denote a range of the standard deviation calculated for 30 samples. The heat cyclic measurement results (b) are shown by the average values for 4 samples.

such changes due to heat treatments are not yet clear, and there is the possibility of a small deflection of the bonded fiber caused by further thermal polymerization of the UV-1100 during longer storage durations. If a criterion for the loss changes was set at ± 1 dB, about 97% of the modulator/fiber bonding would pass, as shown in Fig. 8b. However, it is noted that deterioration of the optical insertion losses due to environmental tests depended not only on the adhesive material, but also strongly on the bonding structure. Mekada *et al*. reported experimental results on unexpectedly large loss increases during heating tests of similar devices with the bonding structure as shown in Fig. 7c, which had a very thick (400 μm) adhesive layer between the bead and chip [3]. The same results were confirmed here and are denoted by closed circles in Figs. 8a and 8b. The bonding layer thicknesses of these 78 modulator devices were broadly distributed within an order from tens to hundreds of micrometers. Of these devices, only 70% of them could pass the criterion of ± 1 dB loss change as shown in Fig. 8b.

Then, a temperature dependence of the change of the optical insertion loss was measured for the fabricated modulators which consisted of the fiber bonding structure as shown in Figs. 7a and 7b. The results measured for 30 devices, which had experienced the environmental tests of Fig. 8, within their ordinary operating temperature increase from 0 to 70℃, are shown in Fig. 9a. The circles and error bars denote the average and the standard deviation ($\pm\sigma_{n-1}$) values, respectively. This temperature dependence was reversible against temperature changes as shown in Fig. 9b, in which the average loss changes during one temperature cycle for four modulators were plotted. Consequently, the fluctuation of the optical insertion losses of the fiber bonding using the UV-1100 materials was within 0.5 dB between 0 and 70℃.

Finally, further environmental tests were carried out for

TABLE 1
Changes of Optical Insertion Losses Due to Various Environmental Tests of Hermetically Packed Ti:$LiNbO_3$ Mach–Zehnder Modulator Devices Assembled Using the UV-1100 Adhesive Material for the Fiber Bonding

Test	Sample	Change of optical Insertion loss average (dB)	σ_{n-1} (dB)
−20°C / +70°C heat cycles ~ 2°C/min, 30 min soaking 1000 cycles	8	−0.32	0.50
−35°C storage for 1000 h	3	−0.02	0.51
40°C, 95% RH damp heat, 56 days	7	−0.12	0.26
80°C, 95% RH damp heat, 200 h	4	0.10	0.57
Mechanical vibrations 20 ~2000 Hz, 20 G, 4 min/cycle, 4 cycles/axis	4	−0.19	0.51
Mechanical shocks 500 G, 0.5 ms, 5 times/axis	4	−0.11	0.15

Note. Unexpectedly large loss increases due to optical fiber breaks in the packages were excluded from these results. No deterioration was observed in the measurements of the optical return losses after the tests.

some of the fabricated modulator devices. The results are summarized in Table 1, suggesting the high mechanical stability of the fiber bondings.

7. CONCLUSION

The new UV-curable adhesive material 'UV-1100' with a refractive index of 1.46, which was obtained from Daikin Industries, Ltd. (Japan), was assessed for its application to the optical fiber bondings in optical device assembly process. The results indicated its chemically and mechanically high stability below 80℃ and demonstrated its practical usage in hermetically sealed devices. This adhesive material was applied here to fabricate hundreds of Ti:$LiNbO_3$ Mach–Zehnder optical intensity modulators, where highly stable and reliable optical coupling characteristics were confirmed within 0 to 70℃.

ACKNOWLEDGMENTS

The authors thank Daikin Industries, Ltd. for the helpful information about the UV-1100, UBE Scientific Analysis Laboratory Co. for the help in chemical analyses, and T. Saito, T. Tateyama, S. Murata, K. Kiuchi, T. Sugimoto, and S. Oikawa of Sumitomo Osaka Cement Co., Ltd. for the help in sample preparation and measurements.

REFERENCES

[1] N. Murata, "UV-curable high reliable adhesive materials." *J. Technol. Transfer,* vol. 15–16, 11 (1992).

[2] Daikin Industries, Ltd., Settsu-shi, Osaka, Japan.

[3] N. Mekada, M. Seino, Y. Kubota, and H. Nakajima, "Practical method of waveguide-to-fiber connection: direct preparation of waveguide endface, by cutting machine and reinforcement using ruby beads," *Appl. Opt*., vol. 29, no. 34, 5096 (1990).